Electronic Supplementary Information

Experimental section

Materials: Iron(III) chloride ($FeCl_3$), terephthalic acid ($C_8H_6O_4$), N, N-dimethylformamide (DMF), disodium phosphate anhydrous (Na_2HPO_4), potassium phosphate monobasic (KH_2PO_4), ethylenediaminetetraacetic acid disodium, potassium hydroxide (KOH), sodium hydroxide (NaOH), and N, N-diethyl-p-phenylenediamine (DPD) were obtained from Shanghai Maclin Biochemical Technology Co., Ltd. Urea, iridium(III) chloride ($IrCl_3$), sodium chloride (NaCl), sodium carbonate (Na_2CO_3), ruthenium oxide (RuO_2), Pt/C (20 wt.% Pt on Vulcan XC-72R), and Nafion (5 wt.%) were bought from Aladdin Ltd. (Shanghai, China). Nickel nitrate hexahydrate ($Ni(NO_3)_2 \cdot 6H_2O$) was obtained from the Tianjin Damao chemical reagent factory. Acetone, ethanol, potassium permanganate ($KMnO_4$), sulfuric acid (H_2SO_4), and hydrochloric acid (HCl) were purchased from Beijing Chemical Reagent Co., Ltd (Beijing, China). Natural seawater was procured from Qingdao, Shandong, China. Before utilization, most magnesium and calcium salts were eliminated by adding Na_2CO_3 to the natural seawater. Ni foam (NF) was obtained from Shenzhen Green and Creative Environmental Science and Technology Co., Ltd. The study employed ultrapure water throughout.

Preparation of NiFe-MOF/NF: The NF (2.0 × 3.0 cm^2) was initially subjected to sonication in HCl, ethanol, and water for 15 minutes each. Solution A is made by mixing $Ni(NO_3)_2 \cdot 6H_2O$ (291 mg) and $FeCl_3$ (81 mg) in 30 ml of distilled water. Terephthalic acid (16.6 mg) was dissolved in 9 ml of DMF as solution B. Then, solutions A and B should be combined and stirred for 30 minutes. The pretreated NF was put into the mixed solution in a Teflon-lined autoclave and heated at 150 °C for 6 h to get NiFe-MOF/NF. Then, it was taken out, washed with water, and dried at 60 °C for 2 h.

Preparation of Ir@NiFe-MOF/NF: Dissolve $IrCl_3$ (26.8 mg) in 30 ml water at 80 °C. Subsequently, the precursor NiFe-MOF/NF was introduced into a reactor with the $IrCl_3$ solution and heated at 80 °C for 12 h. Allow the reactor to cool, then remove the material to wash and dry to obtain Ir@NiFe-MOF/NF.

Preparation of RuO_2/NF and Pt/C/NF: RuO_2 (5 mg) was added to a solution containing Nafion (20 μL), ethanol (490 μL), and water (490 μL) with the aid of ultrasonication (30 min) to form a homogeneous ink (5 mg mL^{-1}). Catalyst ink (100 μL) was then dropped onto a piece of cleaned NF (0.5 × 0.5 cm^2) with a loading mass of 2.0 mg cm^{-2}. Pt/C/NF was prepared in the same way as RuO_2/NF.

Characterizations: X-ray diffraction (XRD) data were obtained using a Philip D8 apparatus with a Cu Kα source (λ = 1.54056 Å). Raman spectroscopy was recorded on the Lab RAM HR Evolution confocal microscope with a 532 nm laser. To examine the morphology and composition of the samples, a scanning electron microscope (SEM, ZISS 300) equipped with energy dispersive X-ray (EDX) facility, a transmission electron microscope (TEM, JEM-F200, JEOL Ltd.) and X-ray photoelectron spectroscopy (XPS, ESCALAB 250 Xi) was utilized.

Electrochemical measurements: All electrochemical tests were conducted using the CHI 660E and 1140C electrochemical workstations. The working electrodes were prepared as described previously and were 0.5 × 0.5 cm^2 in size. The Hg/HgO and graphite rod were used as the reference and counter electrodes. Three distinct electrolytes were employed, comprising 1 M KOH, 1 M KOH + 0.5 M NaCl, and 1 M KOH + seawater, with a pH value of approximately 14.0. All measured potentials were converted to potentials relative to the reversible hydrogen electrode (RHE) following the Nernst equation ($E_{RHE} = E_{Hg/HgO} + 0.059 \times pH + 0.098$ V). The Tafel slope was determined through the application of the Tafel equation. Tafel equation: $\eta = b \log j + a$, where η is overpotential, j is the current density (mA cm^{-2}), and b is the Tafel slope (mV dec^{-1}). Electrochemical impedance spectroscopy measurements were conducted over a frequency range of 10^5 to 0.01 Hz with an amplitude of 5 mV. The double-layer capacitance (C_{dl}) values were obtained utilizing cyclic voltammetry (CV) curves with a scan rate of 20−100 mV s^{-1}. The measured solution resistance was corrected for the iR compensation potential according to equation: $E_{corr.} = E - iR \times 0.85$, where E is the original potential, R is the solution resistance, and i is the corresponding current. All data (except for Figs. 3d, 3e, 3f, 3h, 4d, 4e, 4h, S4, S5, S11, S15, and S16) have been reported with iR compensation.

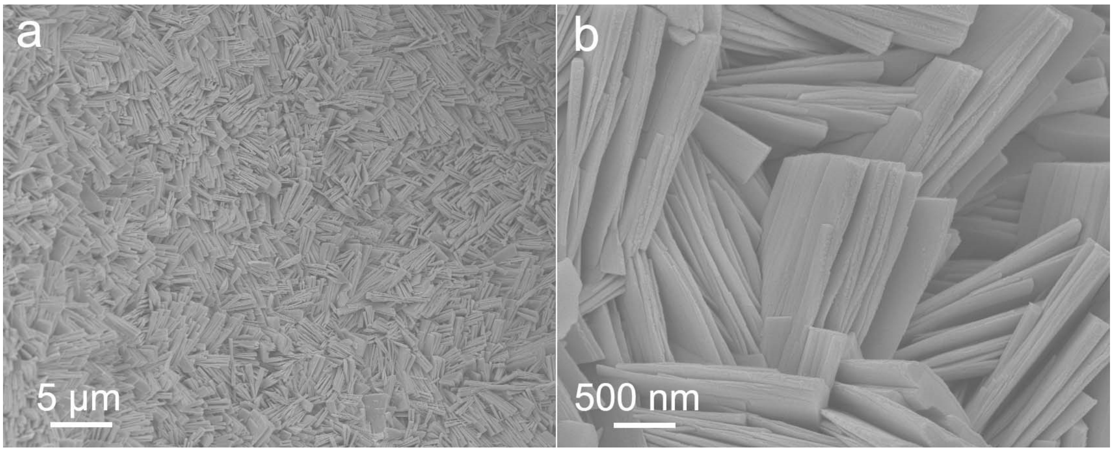

Fig. S1. (a) Low- and (b) high-magnification SEM images of NiFe-MOF/NF.

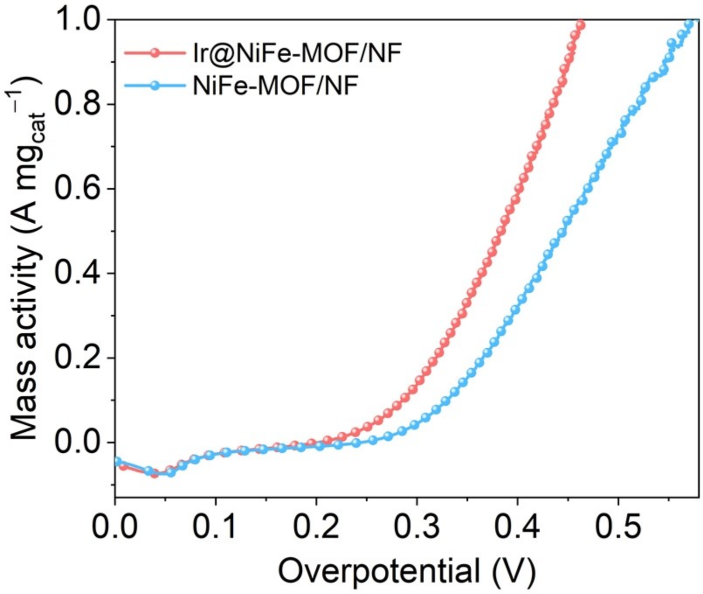

Fig. S2. Mass-normalized LSV curves of Ir@NiFe-MOF/NF and NiFe-MOF/NF in 1 M KOH for OER.

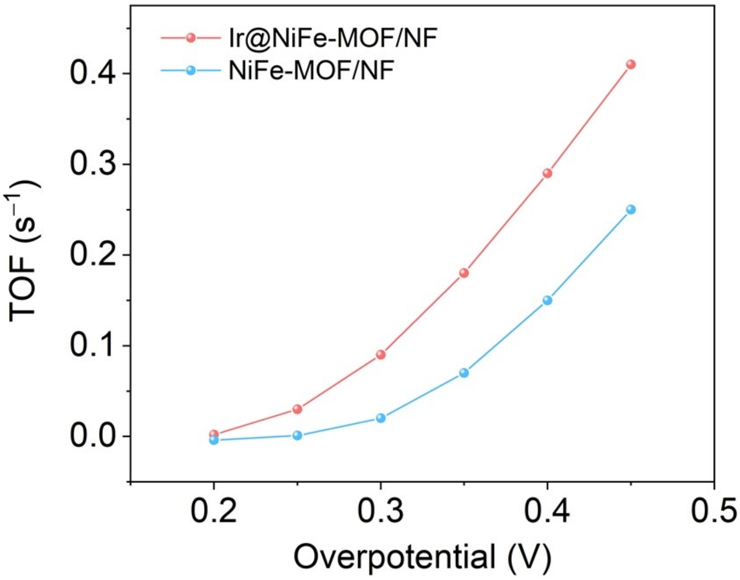

Fig. S3. TOF plots of Ir@NiFe-MOF/NF and NiFe-MOF/NF in 1 M KOH for OER.

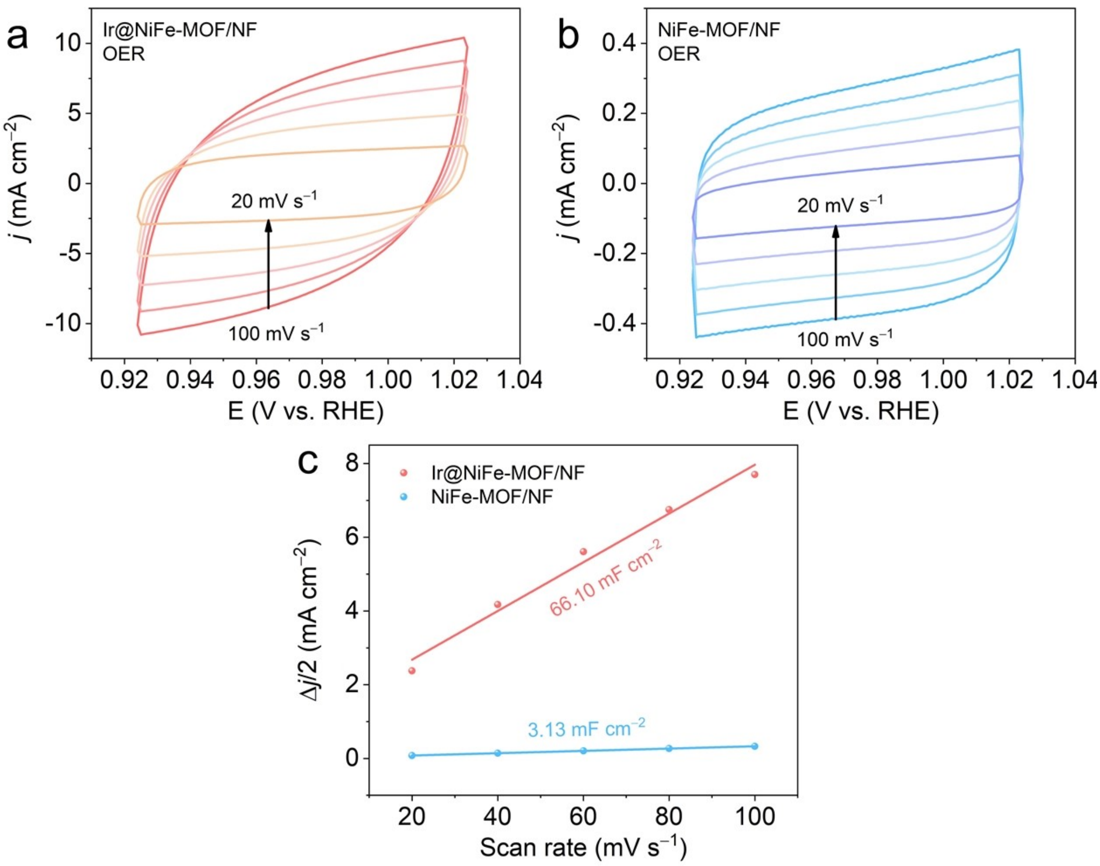

Fig. S4. CV curves of (a) Ir@NiFe-MOF/NF and (b) NiFe-MOF/NF in the double layer region at different scan rates of 20, 40, 60, 80, and 100 mV s^{-1} in 1 M KOH, and (c) C_{dl} values of as-prepared samples for OER.

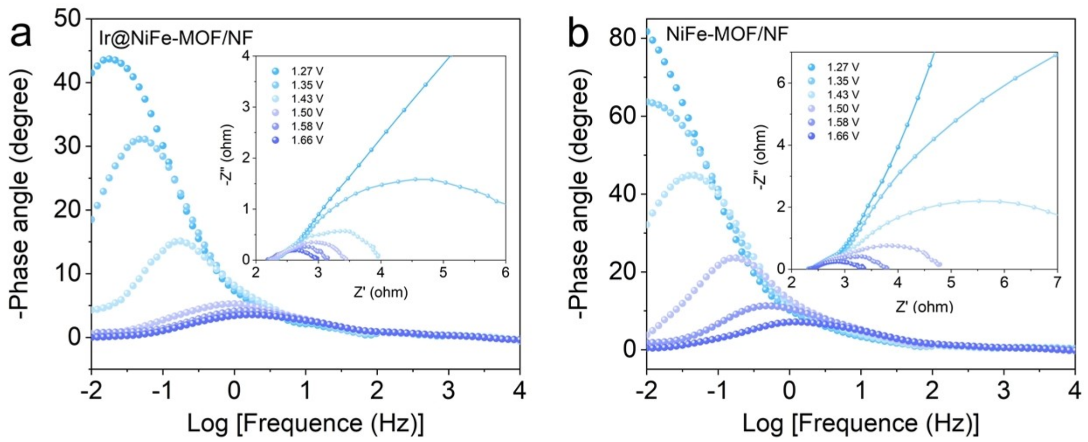

Fig. S5. Operando Nyquist plots and the corresponding Bode phase plots of (a) Ir@NiFe-MOF/NF and (b) NiFe-MOF/NF at different potentials (vs. RHE) for OER.

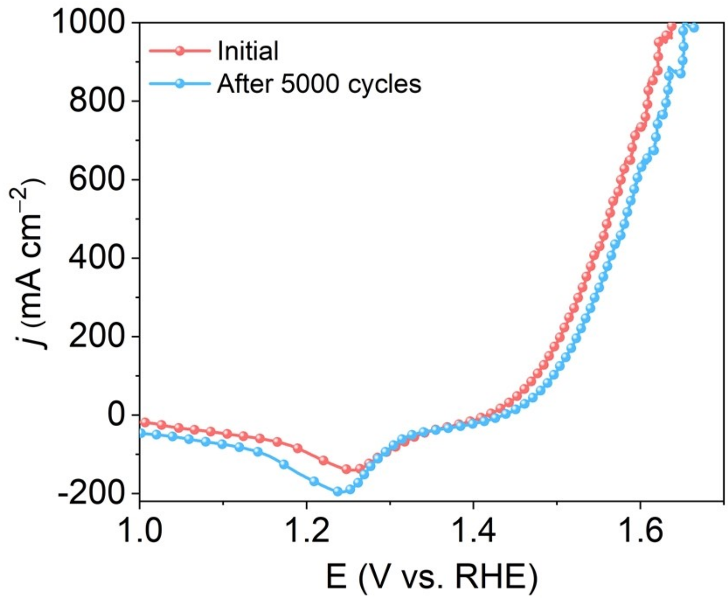

Fig. S6. LSV curves of Ir@NiFe-MOF/NF before and after 5000 CV cycles in 1 M KOH for OER.

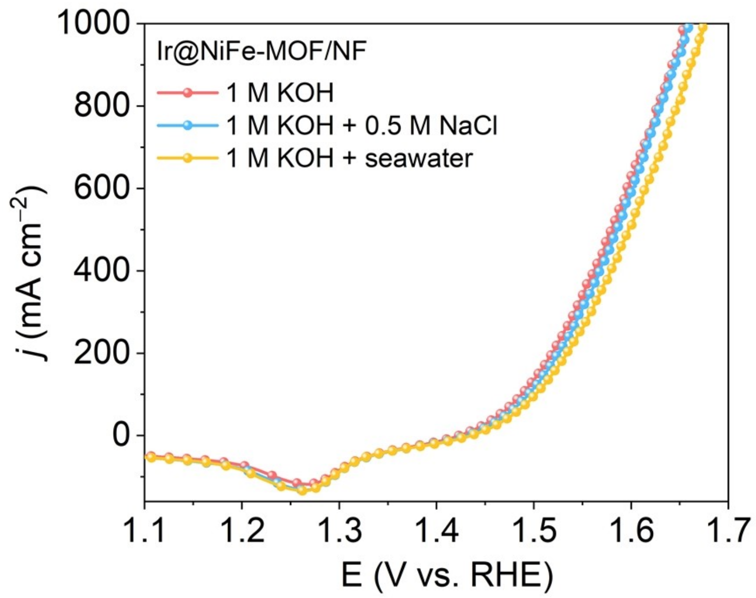

Fig. S7. The LSV curves for the Ir@NiFe-MOF/NF electrode tested in different electrolytes.

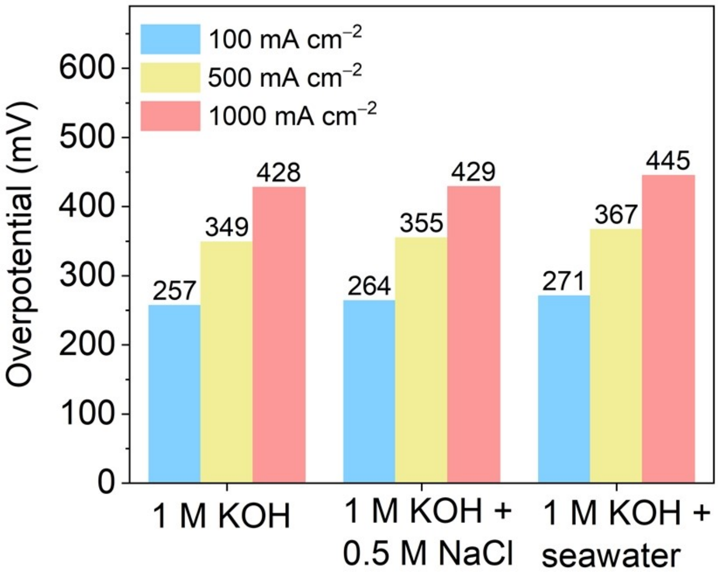

Fig. S8. The corresponding overpotentials for the Ir@NiFe-MOF/NF electrode tested in different electrolytes.

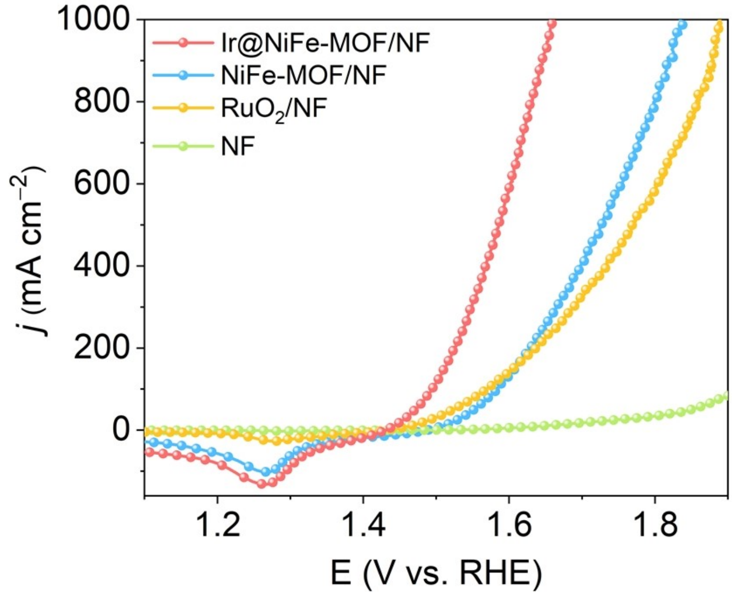

Fig. S9. LSV curves of different catalysts in 1 M KOH + seawater for OER.

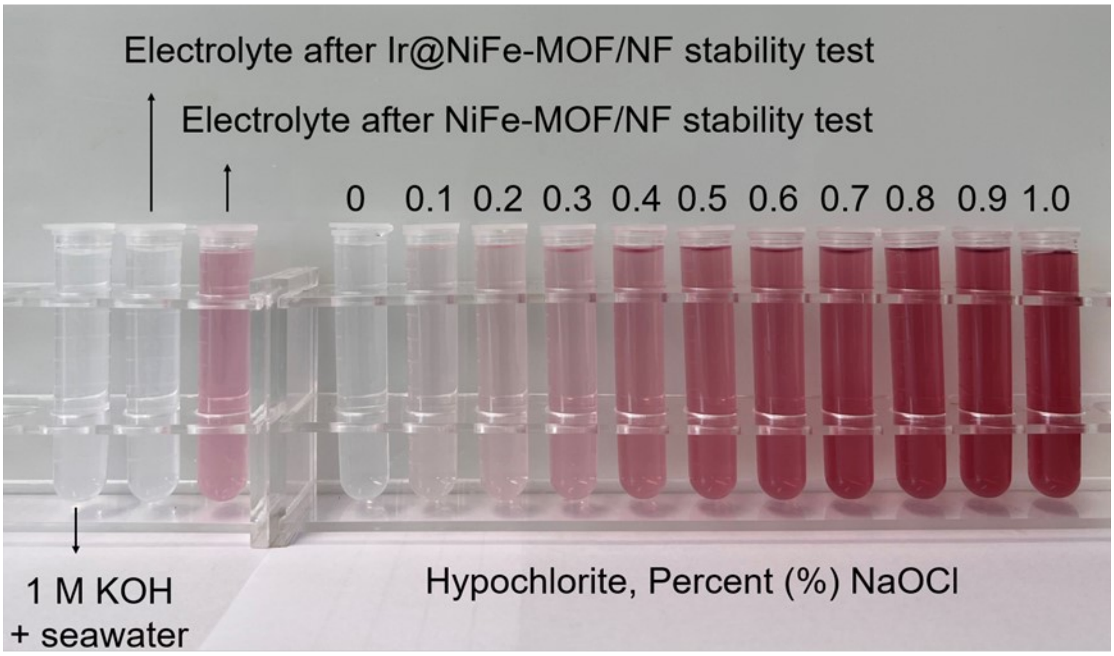

Fig. S10. Hypochlorite detection for the 1 M KOH + seawater electrolyte after stability test.

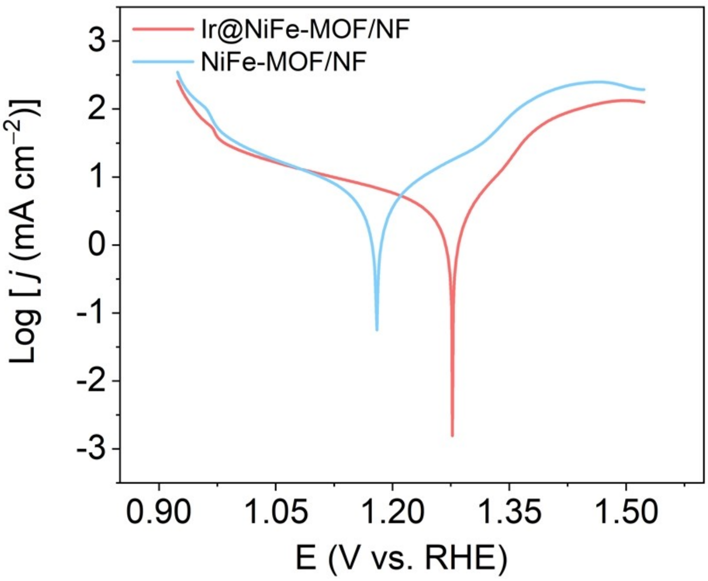

Fig. S11. Tafel plots of Ir@NiFe-MOF/NF and NiFe-MOF/NF in 1 M KOH + seawater.

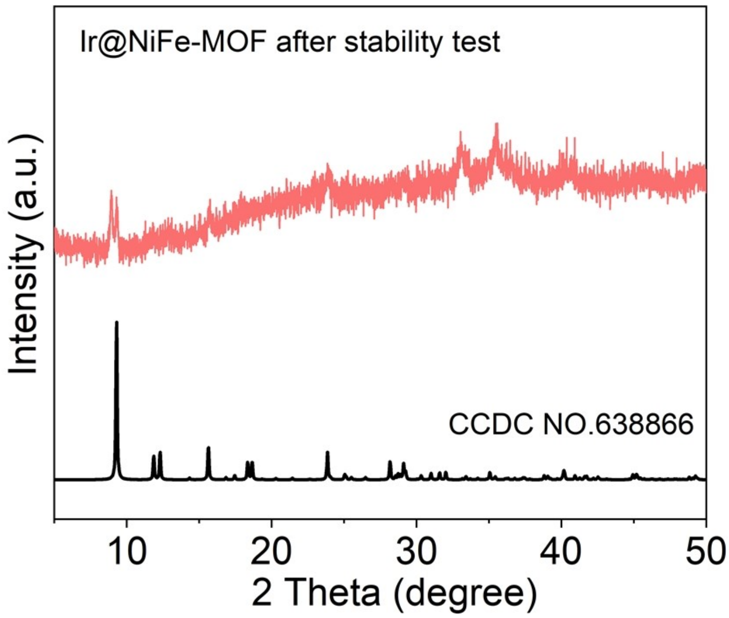

Fig. S12. XRD pattern of Ir@NiFe-MOF after OER stability test.

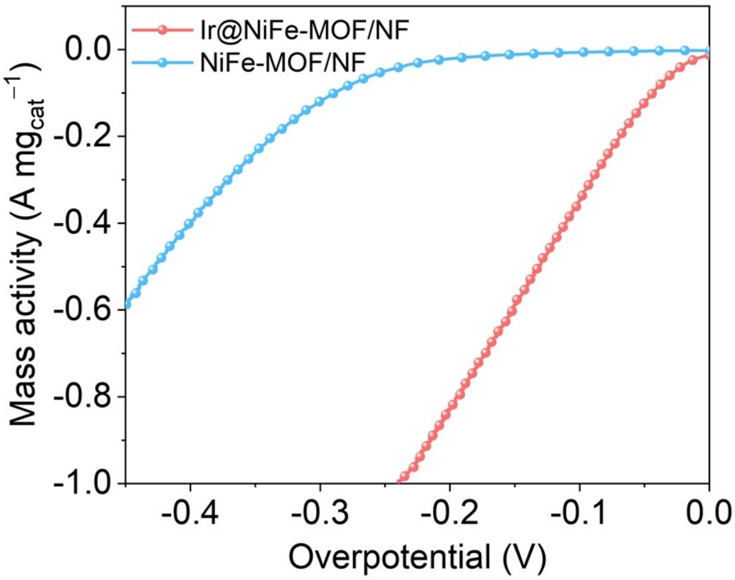

Fig. S13. Mass-normalized LSV of Ir@NiFe-MOF/NF and NiFe-MOF/NF in 1 M KOH for HER.

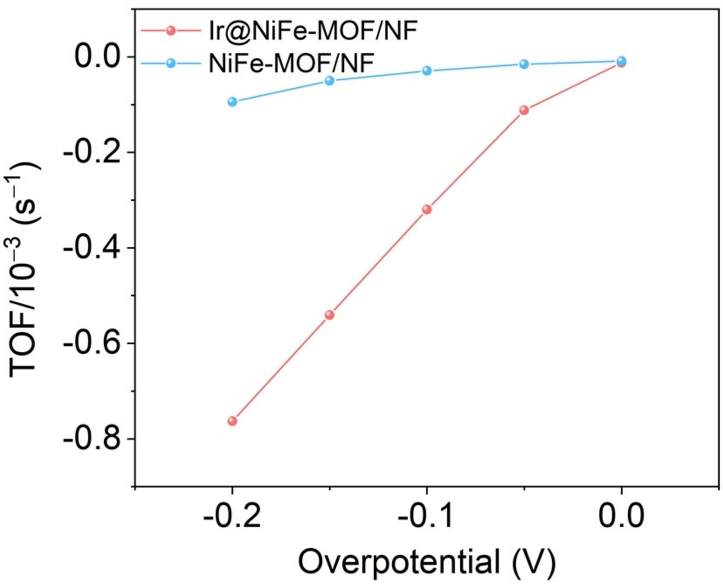

Fig. S14. TOF plots of Ir@NiFe-MOF/NF and NiFe-MOF/NF in 1 M KOH for HER.

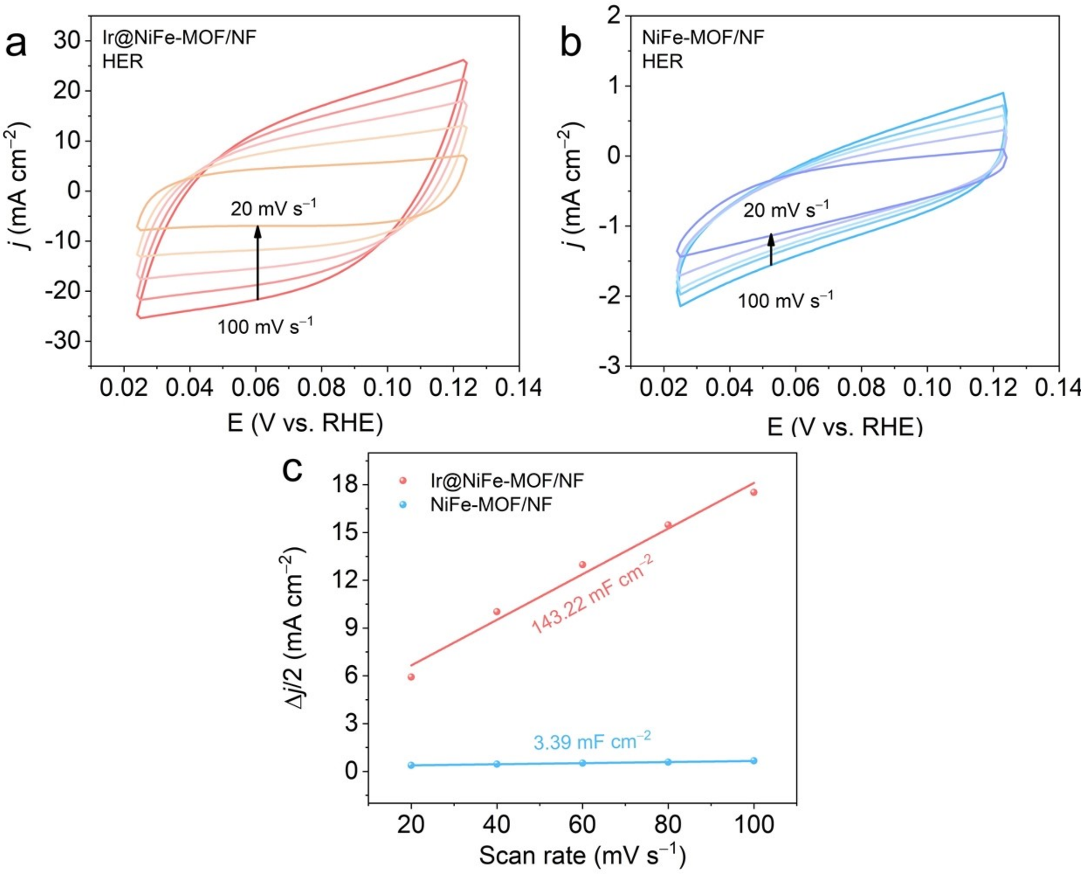

Fig. S15. CV curves of (a) Ir@NiFe-MOF/NF and (b) NiFe-MOF/NF in the double layer region at different scan rates of 20, 40, 60, 80, and 100 mV s^{-1} in 1 M KOH, and (c) C_{dl} values of as-prepared samples for HER.

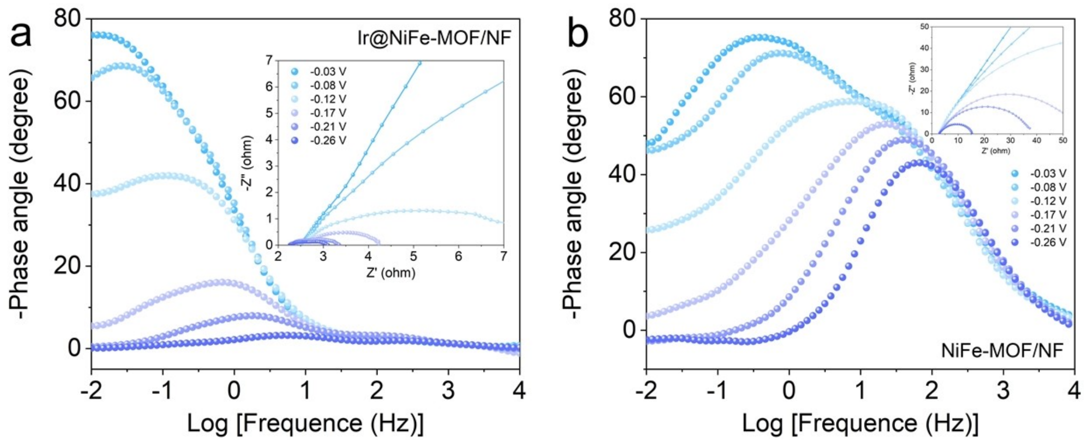

Fig. S16. Operando Nyquist plots and the corresponding Bode phase plots of (a) Ir@NiFe-MOF/NF and (b) NiFe-MOF/NF at different potentials (vs. RHE) for HER.

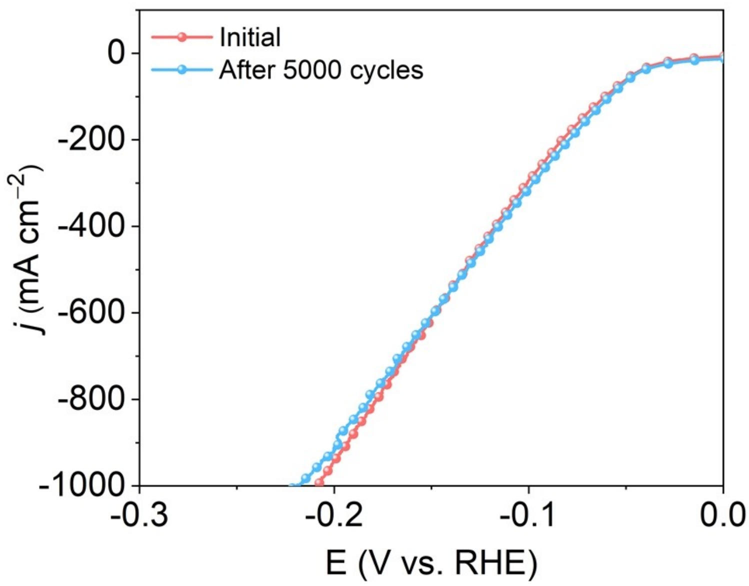

Fig. S17. The LSV curves of Ir@NiFe-MOF/NF before and after 5000 CV cycles in 1 M KOH electrolyte.

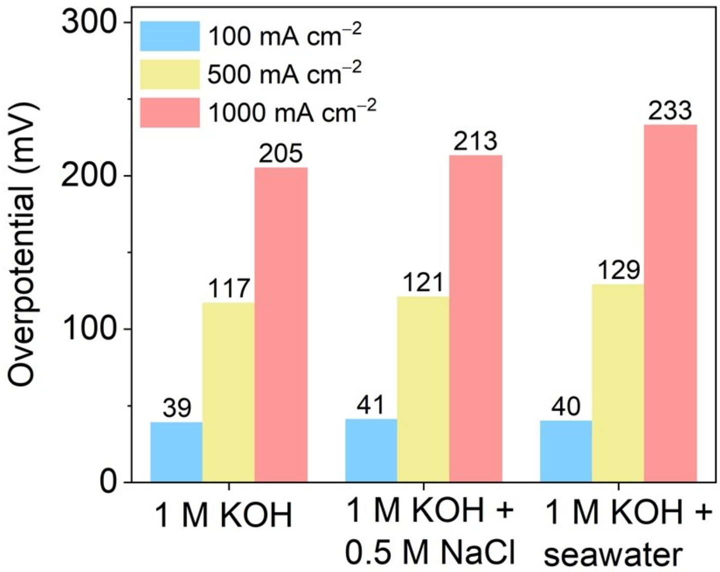

Fig. S18. The HER overpotentials for the Ir@NiFe-MOF/NF electrode tested in different electrolytes.

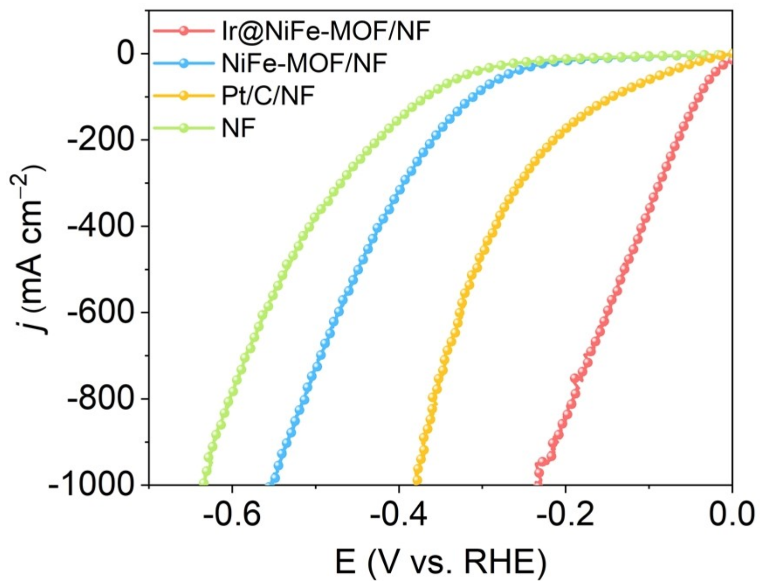

Fig. S19. LSV curves of different catalysts in 1 M KOH + seawater for HER.

Fig. S20. The gas photographs of (a) O_2 and (b) H_2 varying with time at 1000 mA cm^{-2} by drainage method in 1 M KOH + seawater.

Table S1. Element analysis of Ir@NiFe-MOF and NiFe-MOF by ICP-OES.

Element concentration (mg/L)	Ir@NiFe-MOF	NiFe-MOF
Ni	0.184	0.212
Fe	0.043	0.059
Ir	0.433	—

Table S2. Comparison of the OER performance of Ir@NiFe-MOF/NF with other reported OER electrocatalysts.

Catalysts	Electrolyte	Current density (mA cm^{-2})	Overpotential (mV)	Ref.
Ir@NiFe-MOF/NF	**1 M KOH + seawater**	**100**	**271**	**This work**
		500	**367**	
		1000	**445**	
Au/Cr-NiFe/GC	1 M KOH	10	323	*J. Mater. Chem. A*, **2019**, *7*, 9690−9697
NiFe(OH)$_x$@Ni$_3$S$_2$/MoS$_2$-CC	1 M KOH	100	309	*J. Mater. Chem. A*, **2019**, *7*, 2895−2900
Fe-NiCo$_2$O$_4$/NF	1 M KOH	100	350	*Appl. Surf. Sci.*, **2017**, *416*, 371−378
Ni$_{0.3}$Fe$_{0.7}$-LDH@NF	1 M KOH	100	256	*Appl. Catal. B*, **2023**, *323*, 122091
NRAHM-NiO/NF	1 M KOH + seawater	100	340	*ACS Catal.*, **2023**, *13*, 5516−5528
NiPS/NF	1 M KOH + seawater	500	392	*J. Energy Chem.*, **2022**, *75*, 66−73
NiNS/NF	1 M KOH + seawater	100	404	*J. Mater. Chem. A*, **2019**, *7*, 8117−8121
NiCoHPi@Ni$_3$N/NF	1 M KOH + seawater	100	396	*ACS Appl. Mater. Interfaces*, **2022**, *14*, 22061−22070
		500	474	
RuNi-Fe$_2$O$_3$/IF	1 M KOH + seawater	1000	497	*Chin. J. Catal.*, **2022**, *43*, 2202−2211
S-(Ni,Fe)OOH/NF	1 M KOH + seawater	100	300	*Energy Environ. Sci.*, **2020**, *13*, 3439−3446
		500	398	
		1000	462	
NiMoN@NiFeN/NF	1 M KOH + seawater	100	307	*Nat. Commun.*, **2019**, *10*, 5106
NiCoS/NF	1 M KOH + seawater	10	280	*Appl. Catal. B*, **2021**, *291*, 120071
		100	360	
		500	440	
NiFe-LDH-6-4/CC	1 M KOH + seawater	100	301	*Mater. Today Energy*, **2021**, *22*, 100883
Ni$_3$N@C/NF	1 M KOH + seawater	100	314	*J. Mater. Chem. A*, **2021**, *9*, 13562−13569
S-NiFeSe$_2$/NF	1 M KOH + seawater	100	367	*Sci. China Chem.*, **2024**, *67*, 2747−2754
NiCo-EDA/GC	1 M KOH + seawater	100	670	*Electrochim. Acta*, **2017**, *247*, 381−391
Cr-Co$_x$P/NF	1 M KOH + seawater	100	334	*Adv. Funct. Mater.*, **2023**, *33*, 2214081
MoN-Co$_2$N/GC	1 M KOH + seawater	100	357	*ACS Appl. Mater. Interfaces*, **2022**, *14*, 41924−41933
		500	432	

$CoSe_2$-NCF/CC	1 M KOH + seawater	100	455	*Inorg. Chem. Commun.*, **2022**, *146*, 110170
$Ni(OH)_2$-TCNQ/GP	1 M KOH + seawater	100	382	*Nano Res.*, **2022**, *15*, 6084−6090
		500	542	
S-Cu_2O-CuO/CF	1 M KOH + seawater	100	320	*Catal. Today*, **2022**, *400−401*, 14−25
		500	440	
RuMoNi/NF	1 M KOH + seawater	1000	484	*Nat. Commun.*, **2023**, *14*, 3607
RuV-CoNiP/NF	1 M KOH + seawater	100	318	*J. Mater. Chem. A*, **2021**, *9*, 26852−26860
NiFe-PBA-gel-cal/GC	1 M KOH + seawater	100	329	*Adv. Sci.*, **2022**, *9*, 2200146

Table S3. Corrosion potential ($E_{corr.}$) and corrosion current density ($j_{corr.}$) values of Ir@NiFe-MOF/NF and NiFe-MOF/NF.

Catalysts	$E_{corr.}$ (V vs. RHE)	$j_{corr.}$ (mA cm^{-2})
Ir@NiFe-MOF/NF	1.277	3.234
NiFe-MOF/NF	1.180	3.982

Table S4. Comparison of the HER performance of Ir@NiFe-MOF/NF with other reported HER electrocatalysts.

Catalysts	Electrolyte	Current density (mA cm^{-2})	Overpotential (mV)	Ref.
Ir@NiFe-MOF/NF	**1 M KOH + seawater**	**100**	**40**	**This work**
		500	**129**	
		1000	**233**	
(Ni-Fe)S_x/NiFe$(OH)_y$/NF	1 M KOH	100	124	*Appl. Catal. B*, **2019**, *246*, 337−348
NiFe$(OH)_x$@Ni_3S_2/MoS_2-CC	1 M KOH	100	173	*J. Mater. Chem. A*, **2019**, *7*, 2895−2900
NiNS/NF	1 M KOH	100	197	*J. Mater. Chem. A*, **2019**, *7*, 8117−8121
MIL-(IrNiFe)/NF	1 M KOH + seawater	100	79	*J. Mater. Chem. A*, **2021**, *9*, 27424−27433
		500	179	
		1000	235	
Pt-Ni@NiMoN/NF	1 M KOH + seawater	10	11	*Energy Environ. Sci.*, **2023**, *16*, 4584−4592
		100	47	
		500	109	
Pt-hcp Ni NBs/GC	1 M KOH + seawater	10	137	*ACS Appl. Mater. Interfaces*, **2023**, *15*, 51160−51169
NiS@FeNiP/NF	1 M KOH + seawater	100	117	*Small* **2023**, *19*, 2300194
		500	237	
		1000	327	
Fe_x-Ni&$Ni_{0.2}Mo_{0.8}$N/NF	1 M KOH + seawater	10	33	*Energy Environ. Sci.*, **2022**, *15*, 3945−3957
		100	69	
		500	144	
Ni-SN@C/GC	1 M KOH + seawater	10	23	*Adv. Mater.*, **2021**, *33*, 2007508
NiCoHPi@Ni_3N/NF	1 M KOH + seawater	20	87	*ACS Appl. Mater. Interfaces*, **2022**, *14*, 22061−22070
		100	182	
		500	281	
RuNi-Fe_2O_3/IF	1 M KOH + seawater	1000	353	*Chin. J. Catal.*, **2022**, *43*, 2202−2211
Ni-SA/NC	1 M KOH + seawater	10	139	*Adv. Mater.*, **2020**, *33*, 2003846
Ni_2P-Fe_2P/NF	1 M KOH + seawater	100	250	*Adv. Funct. Mater.*, **2021**, *31*, 2006484
CoP_x@FeOOH/NF	1 M KOH + seawater	100	190	*Appl. Catal. B*, **2021**, *294*, 120256
Ni_3N@C/NF	1 M KOH + seawater	100	142	*J. Mater. Chem. A*, **2021**, *9*, 13562−13569
RuV-CoNiP/NF	1 M KOH + seawater	100	103	*J. Mater. Chem. A*, **2021**, *9*, 26852−26860

NiFe-PBA-gel-cal/GC	1 M KOH + seawater	100	480	*Adv. Sci.*, **2022**, *9*, 2200146
npNi/NF	1 M KOH + seawater	100	256	*Inorg. Chem.*, **2024**, *63*, 5773−5778
		1000	352	

Table S5. Comparison of overall water splitting performance for Ir@NiFe-MOF/NF with other reported bifunctional electrocatalysts.

Catalysts	Electrolyte	Current density (mA cm^{-2})	Cell Voltages (V)	Ref.
Ir@NiFe-MOF/NF	**1 M KOH + seawater**	**10**	**1.49**	**This work**
		100	**1.84**	
		500	**2.43**	
$NiFe(OH)_x@Ni_3S_2/MoS_2$-CC	1 M KOH	10	1.55	*J. Mater. Chem. A*, **2019**, *7*, 2895−2900
NiNS/NF	1 M KOH	100	1.93	*J. Mater. Chem. A*, **2019**, *7*, 8117−8121
Ni-SN@C/GC	1 M KOH + seawater	10	1.72	*Adv. Mater.*, **2021**, *33*, 2007508
FCNP@CQDs/CP	1 M KOH + seawater	10	1.61	*Appl. Catal. B*, **2023**, *326*, 122403
Er-MoO_2/NF	1 M KOH + seawater	10	1.52	*Appl. Surf. Sci.*, **2023**, *615*, 156360
FMCO/NF	1 M KOH + seawater	10	1.58	*Appl. Catal. B*, **2023**, *328*, 122488
Mo-CoP_x/NF	1 M KOH + seawater	100	2.16	*Mater. Today, Nano* **2022**, *18*, 100216
Ni@CNTs-Mo_xC/Ni_2P/NF	1 M KOH + seawater	10	1.56	*Nano Energy*, **2023**, *111*, 108440
FeNiCoMnRu@CNT/CP	1 M KOH + seawater	100	2.15	*J. Colloid Interface Sci.*, **2023**, *646*, 844−854
Ru-CoV-LDH/NF	1 M KOH + seawater	100	1.89	*J. Mater. Chem. A*, **2021**, *9*, 26852−26860
$Ru_{22}NiMoP_2$/NF	1 M KOH + seawater	10	1.53	*Sustain. Energy Fuels*, **2023**, *7*, 4677−4686